

# Improving the Gained Power from Solar Chimney by Changing Radius and Height

Nilesh N. Ubhale

M.E. Energy System & Management  
Alamuri Ratnamal Institute of Engg.  
& Technology,  
Sapgoan, India.

E-mail- nileshnubhale@gmail.com

Dr. Lavendra S. Bothra

Principal,  
Alamuri Ratnamal Institute of Engg.  
& Technology,  
Sapgoan, India.

Santosh R Mallah

Department of Mechanical  
Engineering ,  
IIT-BOMBAY, Powai , India.

**Abstract**— This paper evaluates the influence of changing the chimney height and Tower outlet radius and base area on the performance of solar chimney power plant. Results indicate that the chimney height and Tower outlet radius and base area are very important parameters for improving the gained power. In this paper CFD technology is used to investigate the changes in flow kinetic energy caused by the variation of tower flow area with height. It was found that the tower area change affects the efficiency and mass flow rate through the plant. So By changing collector area, chimney tower radius and height it can possible to get maximum efficiency with small change in design of SSCP. Also the simulation convenient to predict the performance of the solar chimney and that can save the cost of the experimental procedures .

**Keywords**- CFD, solar chimney , CFX , solar chimney power plant(SCPP).

\*\*\*\*\*

## I. INTRODUCTION

In the age of globalization demand of energy recourses is increases rapidly while conventional sources of energy are very limited. It also affects the environment adversely. So it is necessary to develop the present renewable sources so that we can satisfy the demand. Solar chimney power plant is one of the best examples of it. By using solar chimney power plant we can produce the large amount of electrical energy as compare to traditional solar energy obtaining equipmentSolar Chimney power technology is a promising large-scale power technology, which absorbs direct and diffused solar radiation and converts parts of solar energy into electric power free of GHG emissions. The solar chimney power plant (SCPP) combines three familiar components: a solar collector, a Solar Chimney situated in the center of the collector, and power conversion unit (PCU) which includes one or several turbine generators.

## II Governing Equations in CFD

There are mainly three equations we solve in computational fluid dynamics problem. They are Continuity equation, Momentum equation (Navier Stokes equation) and Energy equation.

### A . Continuity Equation

$$\frac{\partial \rho}{\partial t} + \frac{\partial(\rho u)}{\partial x} + \frac{\partial(\rho v)}{\partial y} + \frac{\partial(\rho w)}{\partial z} = 0$$

### B. Momentum (Navier Stokes) Equations

$$\rho \left[ \frac{\partial u}{\partial t} + u \frac{\partial u}{\partial x} + v \frac{\partial u}{\partial y} + w \frac{\partial u}{\partial z} \right] = \rho g_x - \frac{\partial p}{\partial x} + \mu \left[ \frac{\partial^2 u}{\partial x^2} + \frac{\partial^2 u}{\partial y^2} + \frac{\partial^2 u}{\partial z^2} \right]$$

$$\rho \left[ \frac{\partial v}{\partial t} + u \frac{\partial v}{\partial x} + v \frac{\partial v}{\partial y} + w \frac{\partial v}{\partial z} \right] = \rho g_y - \frac{\partial p}{\partial y} + \mu \left[ \frac{\partial^2 v}{\partial x^2} + \frac{\partial^2 v}{\partial y^2} + \frac{\partial^2 v}{\partial z^2} \right]$$

$$\rho \left[ \frac{\partial w}{\partial t} + u \frac{\partial w}{\partial x} + v \frac{\partial w}{\partial y} + w \frac{\partial w}{\partial z} \right] = \rho g_z - \frac{\partial p}{\partial z} + \mu \left[ \frac{\partial^2 w}{\partial x^2} + \frac{\partial^2 w}{\partial y^2} + \frac{\partial^2 w}{\partial z^2} \right]$$

### C . Energy Equation

$$\frac{\partial}{\partial t} \left[ \rho \left( e + \frac{1}{2} v^2 \right) \right] + \frac{\partial}{\partial x} \left[ \rho u \left( e + \frac{1}{2} v^2 \right) \right] + \frac{\partial}{\partial y} \left[ \rho v \left( e + \frac{1}{2} v^2 \right) \right] + \frac{\partial}{\partial z} \left[ \rho w \left( e + \frac{1}{2} v^2 \right) \right] =$$

$$k \left( \frac{\partial^2 T}{\partial x^2} + \frac{\partial^2 T}{\partial y^2} + \frac{\partial^2 T}{\partial z^2} \right) - \left( u \frac{\partial p}{\partial x} + v \frac{\partial p}{\partial y} + w \frac{\partial p}{\partial z} \right)$$

$$+ \mu \left[ u \frac{\partial^2 u}{\partial x^2} + \frac{\partial}{\partial x} \left( v \frac{\partial v}{\partial x} + w \frac{\partial w}{\partial x} \right) + v \frac{\partial^2 u}{\partial y^2} + \frac{\partial}{\partial y} \left( u \frac{\partial u}{\partial y} + w \frac{\partial w}{\partial y} \right) + w \frac{\partial^2 u}{\partial z^2} + \frac{\partial}{\partial z} \left( u \frac{\partial u}{\partial z} + v \frac{\partial v}{\partial z} \right) \right]$$

$$+ 2\mu \left[ \left( \frac{\partial u}{\partial x} \right)^2 + \frac{\partial u}{\partial y} \frac{\partial v}{\partial x} + \left( \frac{\partial v}{\partial y} \right)^2 + \frac{\partial v}{\partial z} \frac{\partial w}{\partial y} + \left( \frac{\partial w}{\partial z} \right)^2 + \frac{\partial w}{\partial x} \frac{\partial u}{\partial z} \right] + \rho u g_x + \rho v g_y + \rho w g_z$$

III. 3D Baseline Solar chimney CFD analysis

A . Geometric Model Creation

- Geometries can be created top-down or bottom-up. Top-down refers to an approach where the computational domain is created by performing logical operations on primitive shapes such as cylinders, bricks, and spheres. Bottom-up refers to an approach where one first creates vertices (points), connects those to form edges (lines), connects the edges to create faces, and combines the faces to create volumes. Geometries can be created using the same pre-processor software that is used to create the grid, or created using other programs (e.g. CAD, graphics). Geometry files are imported into HM to create computational domain. The Extracted fluid domain of Solar chimney as shown in Fig . 1

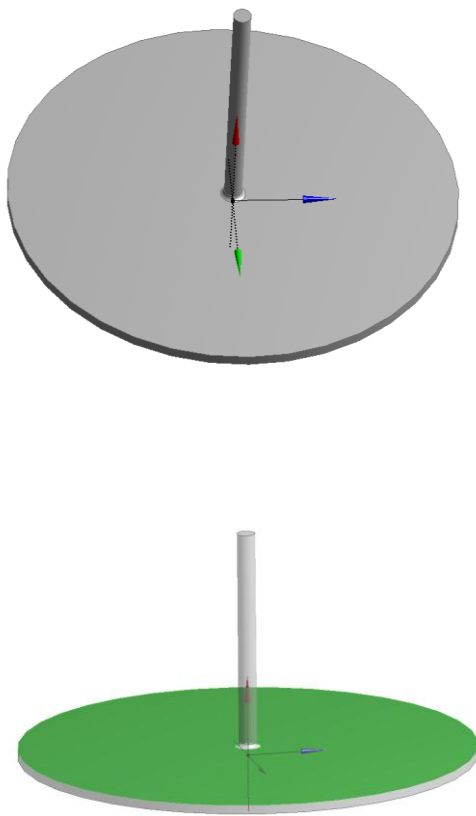


Fig. 1 CFD Model of Solar chimney [15]

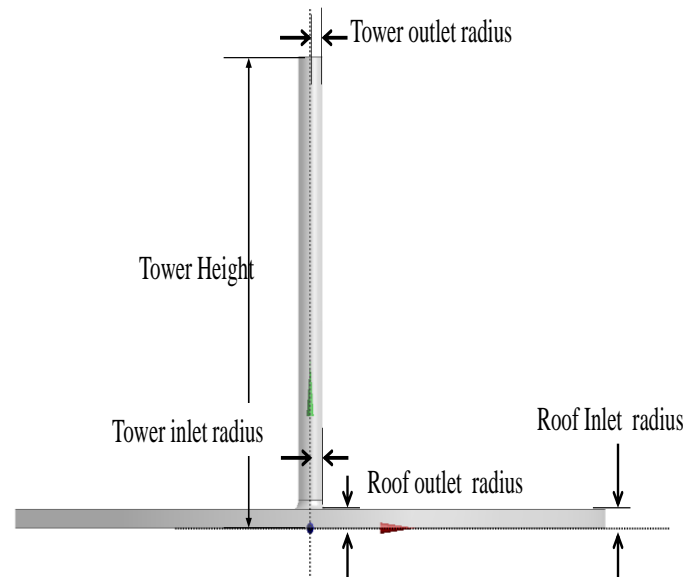


Fig. 2 Solar Chimney nomenclature [15]

B . Mesh generation

A hybrid mesh is generated using Hyper Mesh preprocessor.

- Many different cell/element and grid types are available. Choice depends on the problem and the solver capabilities.
- Cell or element types:

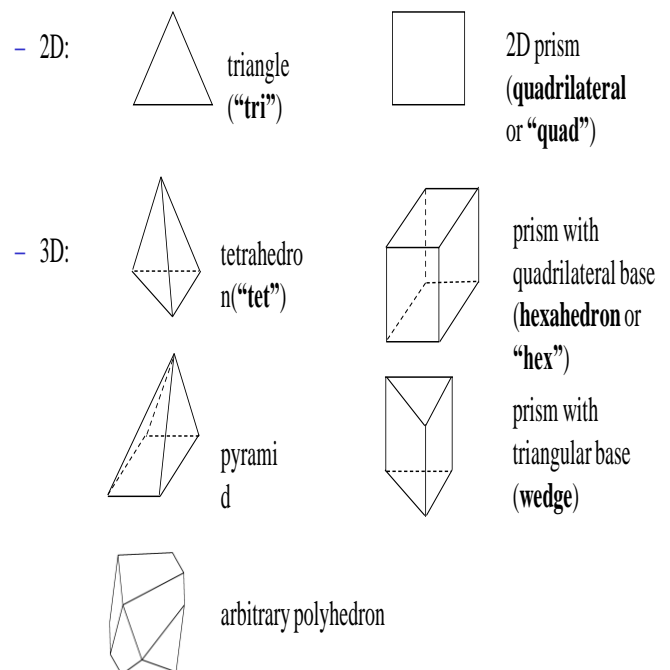


Fig. 3 Cell or element types [15]

First, the surface of the solar chimney is meshed with QUAD element. Then the QUAD element is revolved for 1degree. No of elements is used for all the models 10 thousands. For the mesh generation special care has been taken to the zones close to the walls. In the proximity of the crest the mesh is finer than any other part of the domain. The domain has been subdivided into growing boxes to make it easier to generate the grid. The choice for the elements has been both Prism and hexahedral mesh volumes.

Representations of the different meshes that take part in the study are depicted in the following detailed figures.



Total No of elements= 10 thousands

Fig.4 CFD Domain Mesh [15]

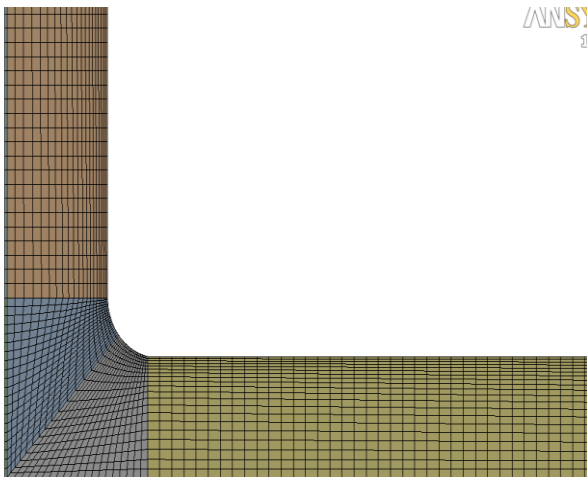


Fig.5 Close View of solar chimney mesh

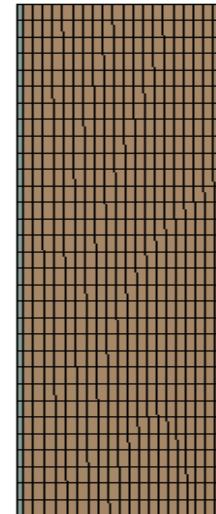


Fig.6 Close View of outlet Mesh

#### . C . Convergence Criteria

The iterative process is repeated until the change in the variable from one iteration to the next becomes so small that the solution can be considered converged.

- At convergence:
  - All discrete conservation equations (momentum, energy, etc.) are obeyed in all cells to a specified tolerance.
  - The solution no longer changes with additional iterations.
  - Mass, momentum, energy and scalar balances are obtained.

Residuals measure imbalance (or error) in conservation equations. The convergence of the simulations is said to be achieved when all the residuals reach the required convergence criteria. These convergence criteria are found by monitoring the in the drag. The convergence criterion for the continuity equation is  $1E-4$  and it is set to  $1E-3$  for the momentum,  $k$  and  $\omega$  equations. The convergence of the residuals is shown in Fig.6.9.

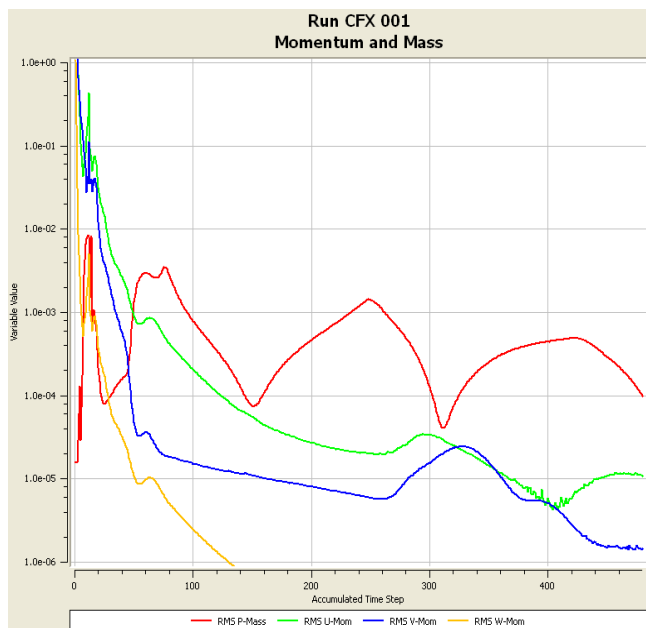


Fig. 7 Convergence criteria Figures and Tables

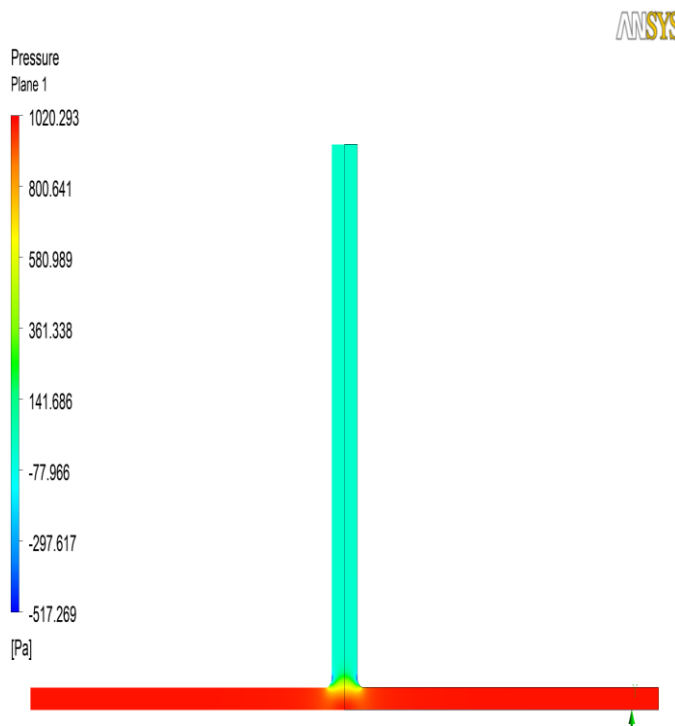


Fig.9 Contours of static Pressure at Mid plane

III. Optimization - Tower outlet radius variation

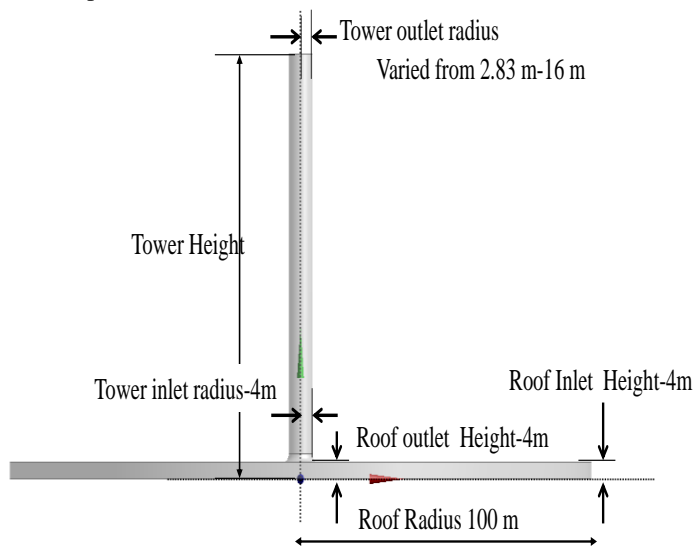


Fig. 8 Tower outlet radius variation

A. Outlet Radius=2.83

In Fig. 9, the gauge pressure distributions are seen to be nominally constant under the roof before falling gradually in the tower portion to meet the hydrostatic pressure value at the tower top. In 10 and 12 the velocity increases as it approaches the tower base and maximum velocity is 45m/s [15].

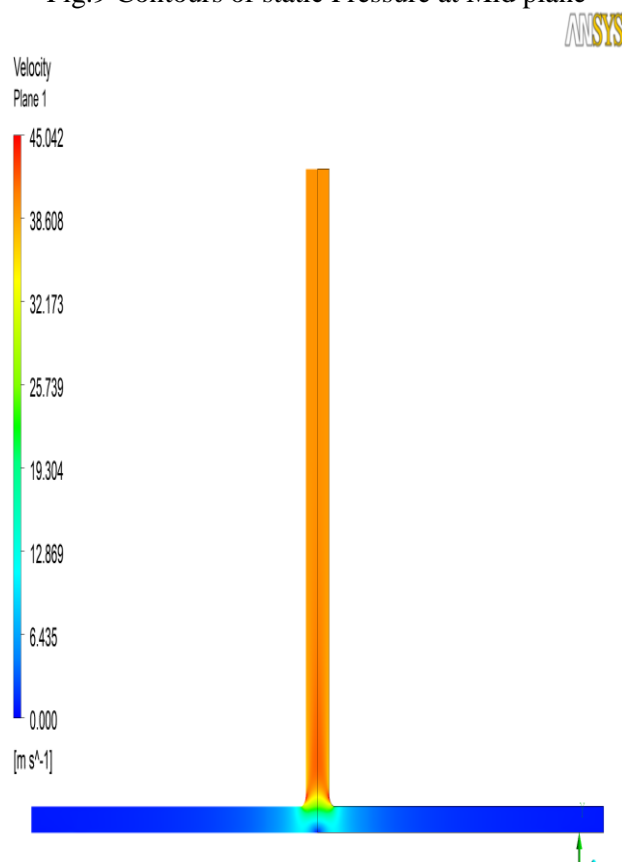


Fig.10 Contours Velocity at Mid plane

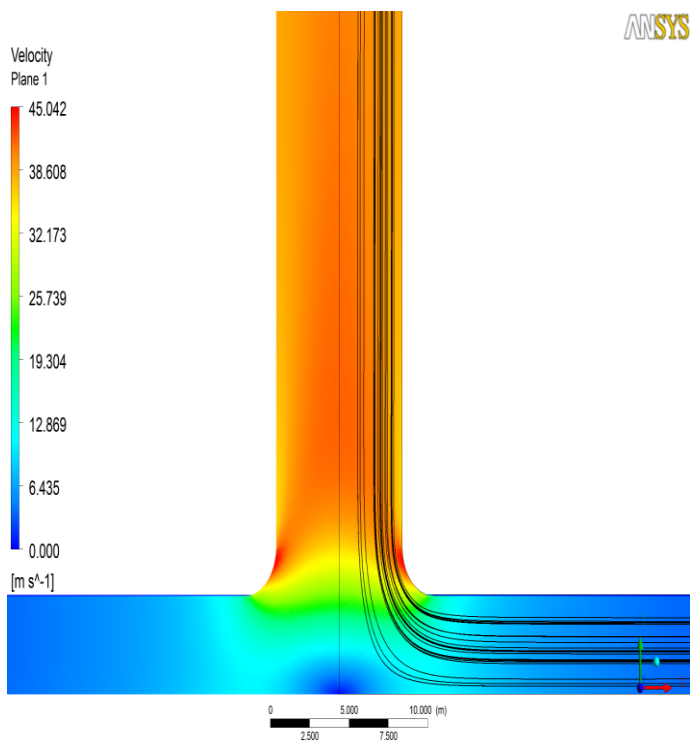


Fig.11 Contours of Velocity Magnitude with streamlines at Mid plane

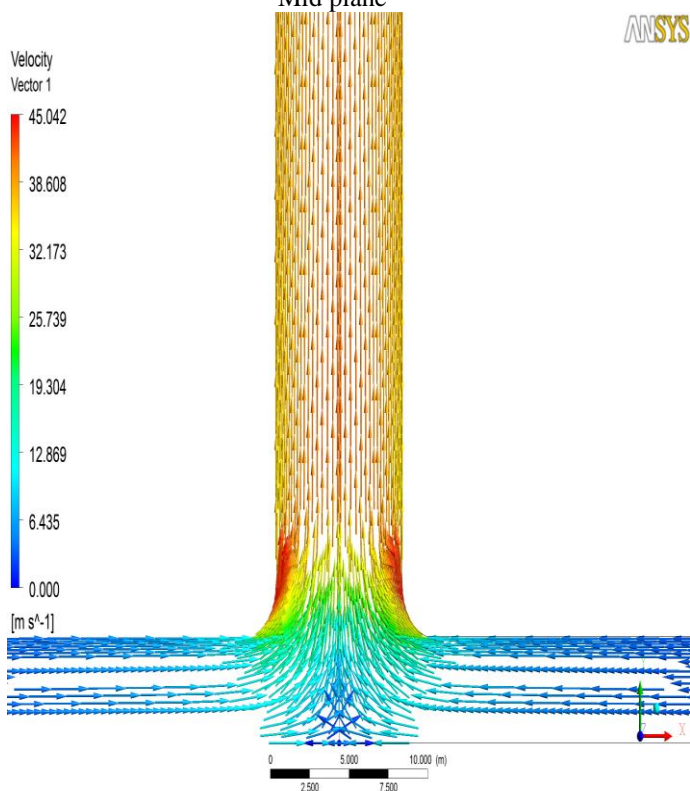


Fig.12 Contours of Velocity vectors  
 B . Outlet Radius = 5.66

In Fig. 13 , the gauge pressure distributions are seen to be nominally constant under the roof before falling gradually in the tower portion to meet the hydrostatic pressure value at the tower top. In 14 and 15 the velocity increases as it approaches the tower base and maximum velocity is 109 m/s. So compared to convergent, outlet divergent is increasing the velocity at tower base [15].

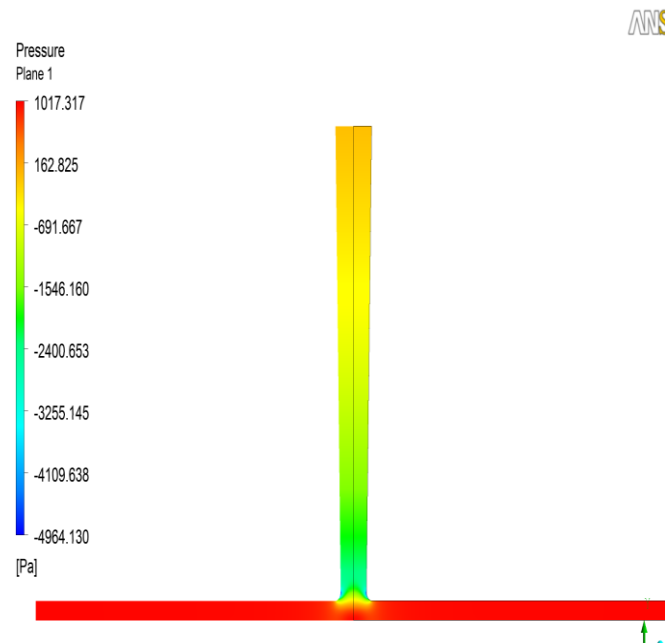


Fig.13 Contours of static Pressure at mid plane

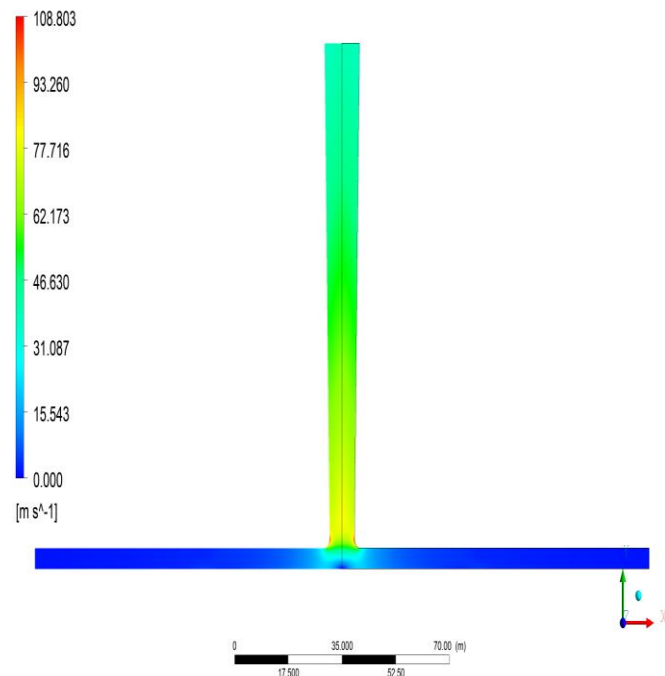


Fig.14 Contours Velocity at mid plane

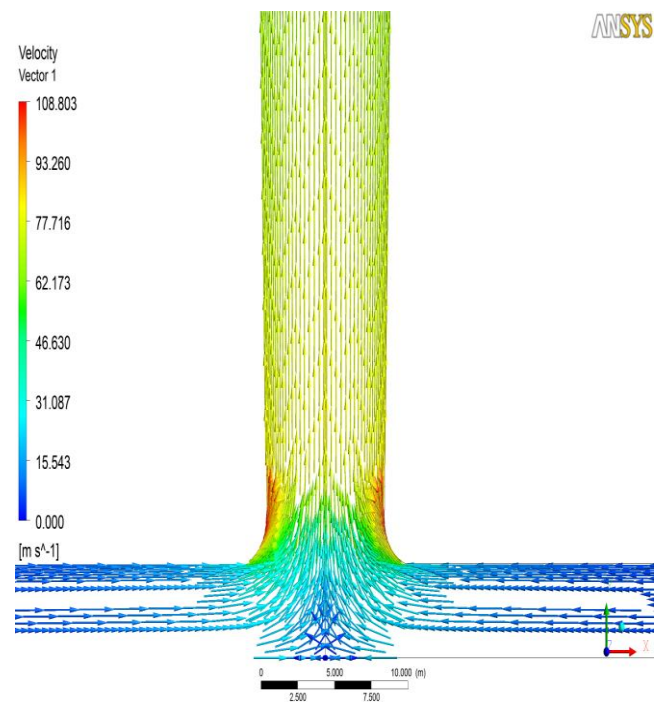
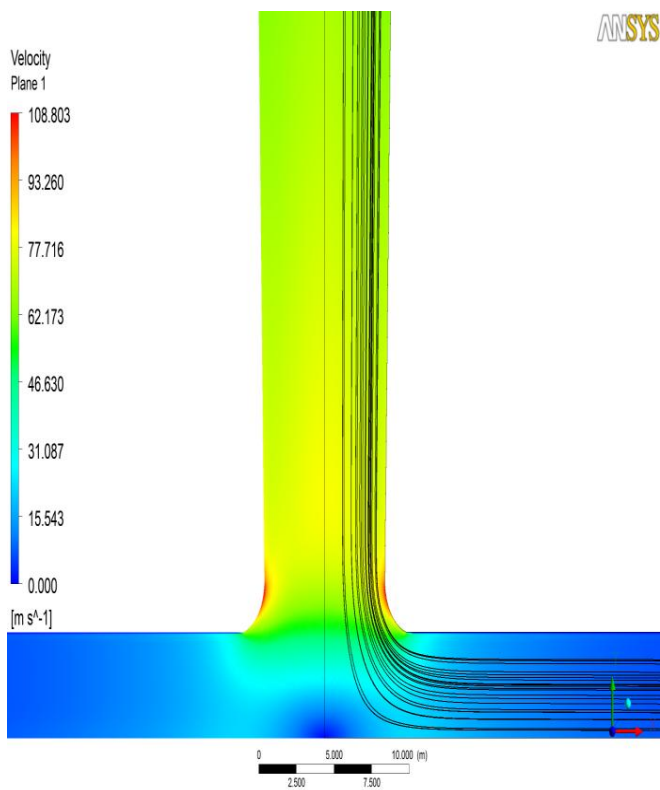


Fig.16 Contours of Velocity vectors

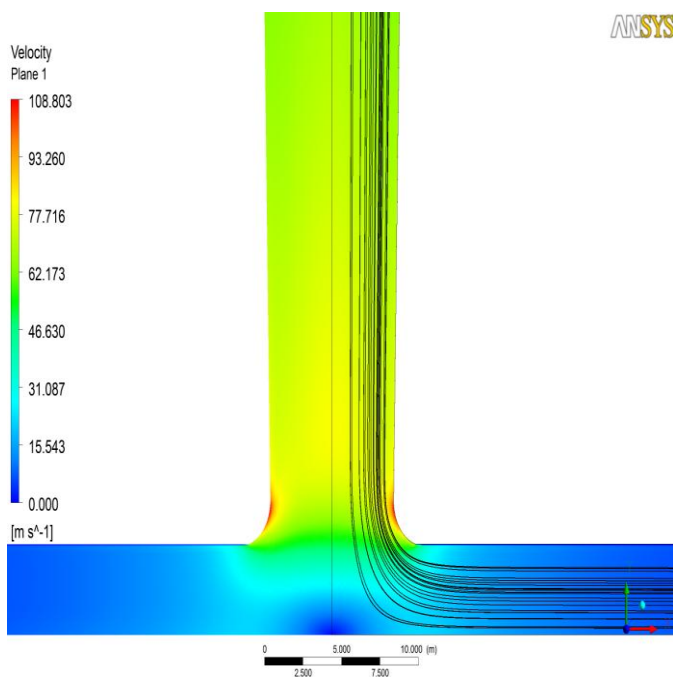


Fig.15 Contours of Velocity Magnitude with streamlines at mid plane

C . Outlet Radius =12

In Fig. 17 , the gauge pressure distributions are seen to be nominally constant under the roof before falling gradually in the tower portion to meet the hydrostatic pressure value at the tower top. In Fig. 18 and Fig. 19 the velocity increases as it approaches the tower base and maximum velocity is 230 m/s. So compared to convergent, outlet divergent is increasing the velocity at tower base [15].



Fig.17 Contours of static Pressure at mid plane

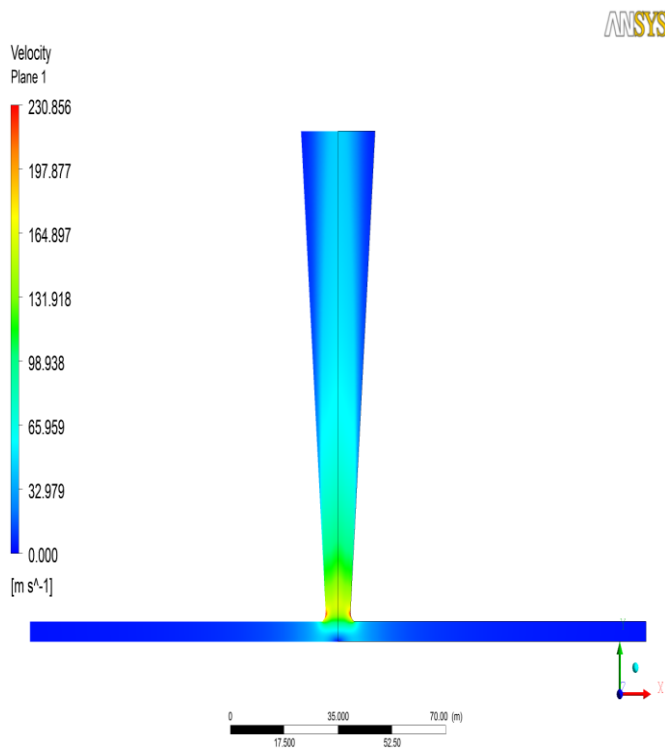


Fig.18 Contours Velocity at mid plane

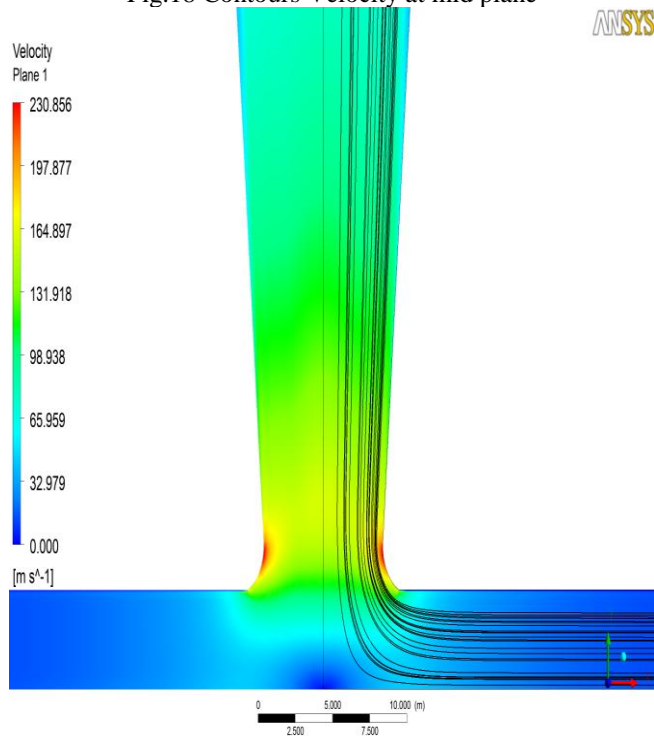


Fig.19 Contours of Velocity Magnitude with streamlines at mid plane

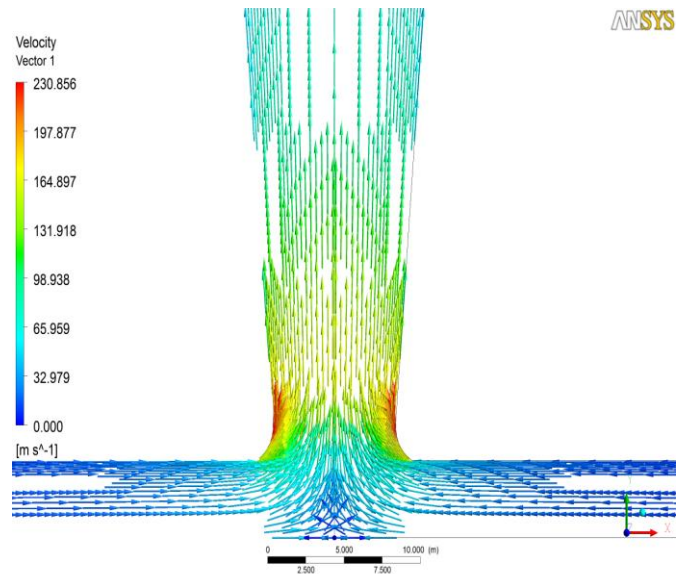


Fig.20 Contours of Velocity vectors

D . Outlet Radius = 16

In Fig. 21 , the gauge pressure distributions are seen to be nominally constant under the roof before falling gradually in the tower portion to meet the hydrostatic pressure value at the tower top. In Fig. 22 and Fig. 23 the velocity increases as it approaches the tower base and maximum velocity is 159 m/s. So compared to convergent, outlet divergent is increasing the velocity at tower base [15].



Fig.21 Contours of static Pressure at mid plane

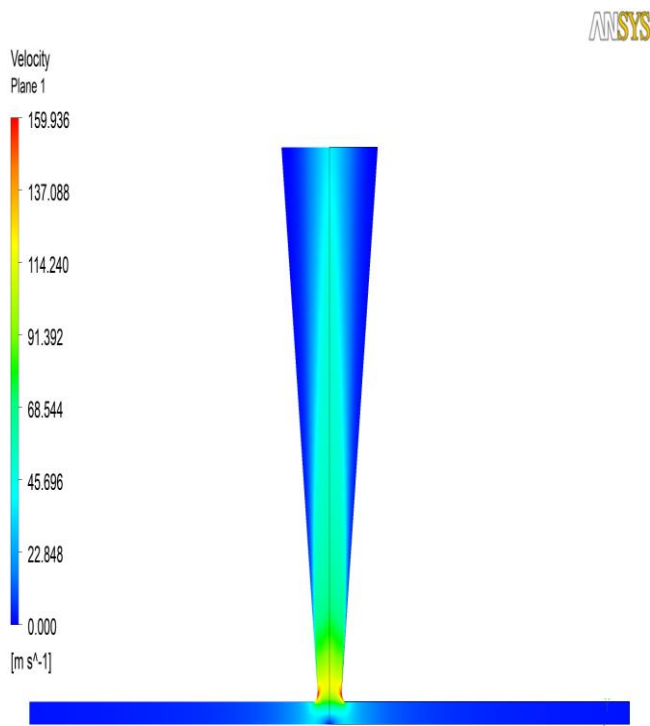


Fig.22 Contours Velocity at mid plane

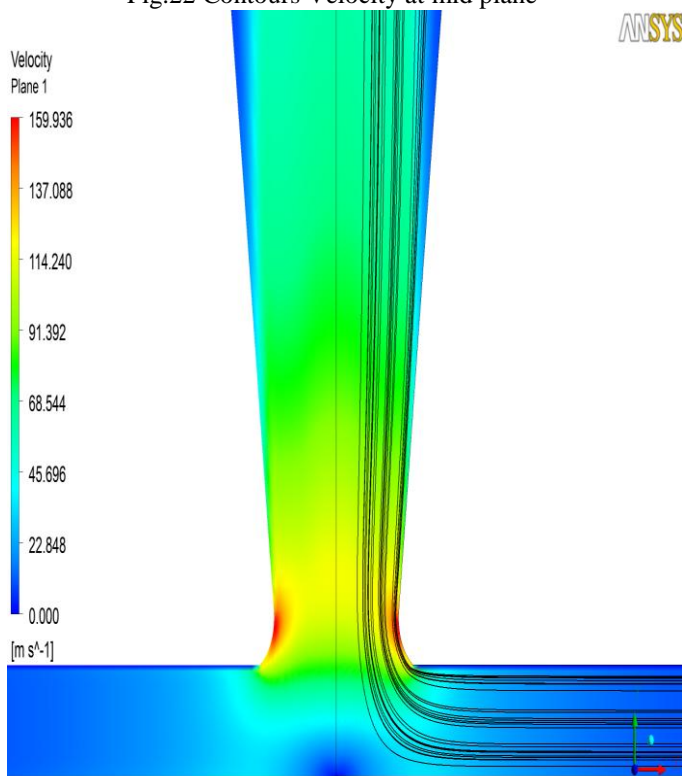


Fig.23 Contours of Velocity Magnitude with streamlines at mid plane

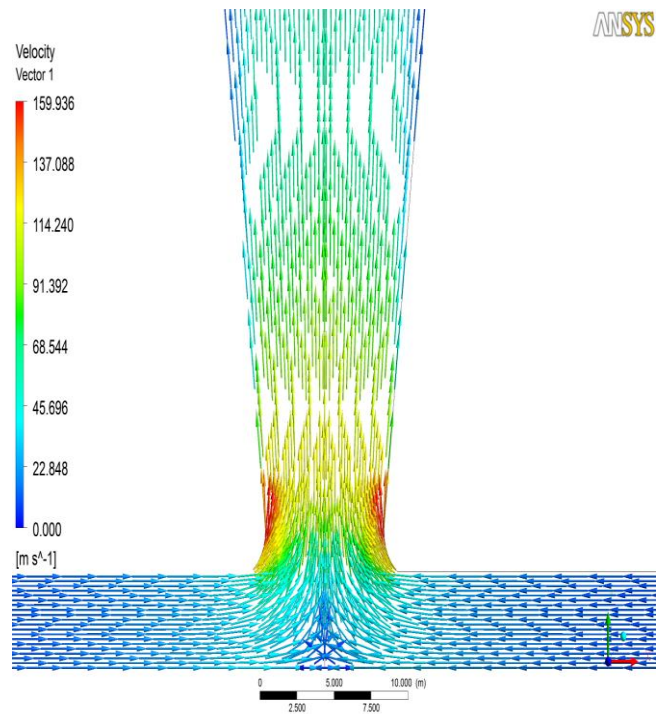


Fig.24 Contours of Velocity vectors

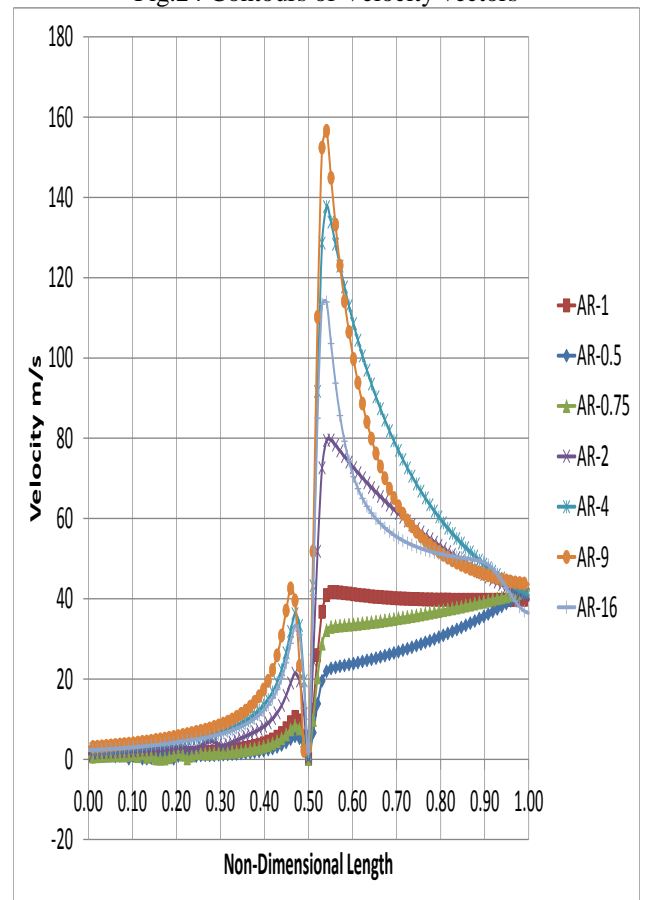


Fig.25 Comparisons of velocity at different Area Ratio

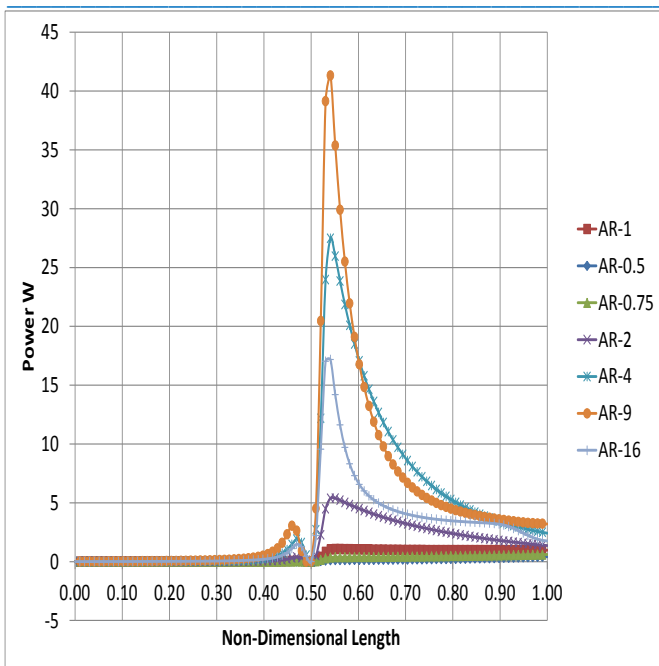


Fig.26 Comparisons of Power at different Area Ratio

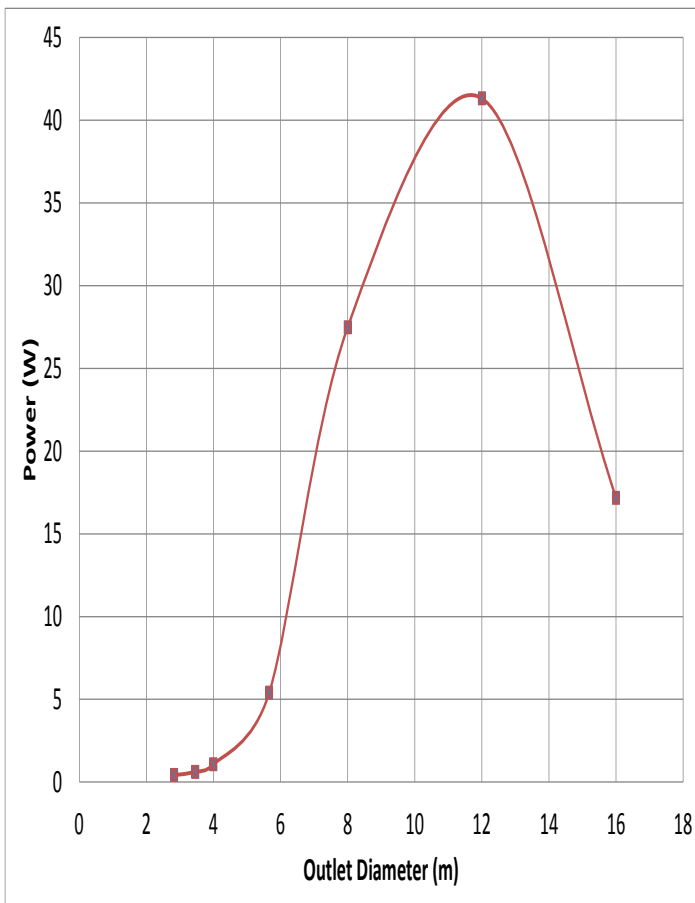


Fig.27 Effect of tower area ratio on Power for insulation = 800 W/m<sup>2</sup>

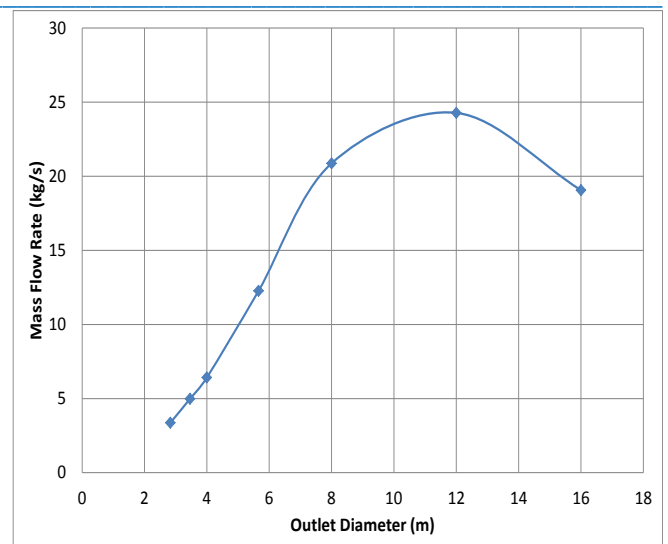


Fig.28 Effect of tower area ratio on the mass flow rate for insulation = 800 W/m<sup>2</sup>

#### IV. CONCLUSION

The results shows that the chimney height and Tower outlet radius and base area are very important parameters for improving the gained power, So compared to convergent, outlet divergent is increasing the velocity hence mass flow rate at tower base. Maximum velocity occurs for a area ratio of 9 as seen from result IV.C(for outlet radius = 12 m , and inlet radius = 4 m) velocity attains its optimum value then with further increase in outlet radius for a given inlet radius there is decrease in velocity at the tower base(can be seen from result IV.D )The results compared with some experimental data from other results researchers and there is a good agreement between simulated and calculated results.

#### REFERENCES

- [1] Schlaich J, Bergermann R, Schiel W, Weinrebe G. "Design of commercial solar updraft tower systems—utilization of solar induced convective flows for power generation". *J Solar Energy Eng* 2005; 127:117–24.
- [2] S.Beerbaum, G.Weinrebe, Solar thermal power generation in India- a techno-economic analysis. *J Renewable Energy* 21(2000) 153-174.
- [3] Y.J. Dai, H.B. Huang and R.Z. Wang, Case study of solar chimney power plants in northwestern regions of China, *J Renewable energy* 28(2003) 1295-1304.
- [4] M.A. dos S. Bernardes, A. Vow and G. Weinrebe, Thermal and technical analysis of solar chimneys, *J Solar Energy* 75(2003) 511-524.
- [5] J.P.Pretorius and D.G. Kroger, Critical evaluation of solar chimney power plant performance, *J Solar Energy* 80(2006) 535-544.
- [6] Xinping Zhou, Jiakuan Yang, Bo Xiao & GuoxiangHou, Simulation of a pilot solar chimney thermal power

- generating equipment, J Renewable Energy 32(2007) 1637-1644.
- [7] AtitKoonsrisuk&TawitChitsomboon, Dynamic similarity in solar chimney modeling, J Solar Energy 81(2007) 1439-1446.
- [8] T.P. Fluri, J.P. Pretorius, C. Van Dyk, T.W. Von backstrom, D.G. Kroger, G.P.A.G. Van Ziji, Cost analysis of solar chimney power plants, J Solar Energy 83(2009) 246-256.
- [9] Xinping Zhou, Jiakuan Yang, Bo Xiao, GuoxiangHou& Fang Xing, Analysis of chimney height for solar chimney power plant, J Applied Thermal Engineering 29(2009) 178-185.
- [10] Cristiana B. Maia, André G. Ferreira, Ramón M. Valle &Marico F.B. Cortez, Theoretical evaluation of the influence of geometric parameters and materials on the behavior of the airflow in a solar chimney, J Computers & Fluids 38(2009) 625-636.
- [11] Tingzhen Ming, Wei Liu, Yuan Pan &GuoliangXu, Numerical analysis of flow and heat transfer characteristics in solar chimney power plants with energy storage layer, J Energy conservation and management 49(2008) 2872-2879.
- [12] Marco Aurelio dos Santos Bernardes, T.W. Von Backstrom & D.G. Kroger, Analysis of Some available heat transfer coefficients applicable to solar chimney power plant collector, J Solar Energy 83(2009) 264-275.
- [13] S. Nizetic, N. Ninic & B. Klarin, Analysis and feasibility of implementing solar chimney power plants in the Mediterranean region, J Energy 33(2008) 1680-1690.
- [14] AtitKoonsrisuk&TawitChitsomboon, Partial geometric similarity for solar chimney power plant modeling, J Solar Energy 83(2009) 1611-1618.
- [15] Jagadeesh.S.Pattanashetti, Madhukeshwara.N, "Numerical Investigation and Optimization of Solar Tower Power Plant",IJRAME, Vol.2 Issue.1,January 2014.Pgs: 92-104.



Nilesh Namdeo Ubhale received his B.E. degree in Mechanical Engineering from “Yadavrao Tasgaonkar Institute of Engineering and Technology”, Mumbai, India, in 2013, He is persuing M.E. in “Energy System and Management” at “Alamuri Ratnamala Institute of Engineering and Technology”, Sapgoan, Maharastra. His research interests include “Numerical Simulation for Solar Chimney by Changing its Radius and Height”